JOURNAL OF THERMOPHYSICS AND HEAT TRANSFER
Vol. 9, No. 3, July–September 1995

Modeling Transient Conduction from Isothermal Convex Bodies of Arbitrary Shape

M. M. Yovanovich,* P. Teertstra,† and J. R. Culham‡
University of Waterloo, Waterloo, Ontario N2L 3G1, Canada

A simple analytical model is developed to predict transient heat conduction from isothermal convex bodies into an infinitely large, constant property surrounding region. The proposed model is based on the linear superposition of two asymptotes, corresponding to transient diffusion into a half-space and steady-state conduction into a full-space. A wide range of body shapes are considered, including oblate and prolate spheroids and various cuboids and infinitely thin bodies. Since simple analytical solutions exist only for the half-space and sphere problems, validation of the proposed model for all other body shapes implements results from numerical solutions over a full range of dimensionless time. The maximum difference between the proposed analytical model and the numerical results for most body shapes occurs in the transition region, $10^{-3} < Fo < 10^{-1}$, and is less than 10%. This maximum difference can be reduced to within 2% by introducing a blended solution for each body shape.

Nomenclature

A	=	active body surface area, m^2
AR	=	body aspect ratio, height/diameter
a	=	focal length, spheroid bodies, m
b	=	sphere radius, m
C_{1-4}, C_S, D	=	finite volume coefficients
c_p	=	specific heat, J/kgK
$Fo_{\sqrt{A}}$	=	Fourier number, $\equiv \alpha t/(\sqrt{A})^2$
g_{11}, g_{22}, g_{33}	=	metric coefficients
i, j	=	control volume indices
k	=	thermal conductivity, W/mK
$\mathscr{L}$	=	characteristic body length, m
n	=	blending parameter
Q	=	instantaneous heat flow rate, W
$Q^*_{\sqrt{A}}$	=	dimensionless heat flow rate,
r, θ, z	=	polar coordinates
r	=	generalized radial coordinate, m
$S^*_{\sqrt{A}}$	=	conduction shape factor
s_1, s_2, s_3	=	cuboid side half-lengths, m
T	=	temperature, °C
t	=	time, s
V	=	body volume, m^3
x, y, z	=	Cartesian coordinates
α	=	thermal diffusivity, m^2/s
$\Delta\eta, \Delta\theta$	=	control volume intervals
η, θ, ψ	=	spheroidal coordinates
θ_0	=	surface temperature difference, $\equiv T_0 - T_\infty$
ρ	=	mass density, kg/m^3
τ	=	dimensionless time, $\equiv \alpha t/\mathscr{L}^2$
ϕ	=	dimensionless temperature, $\equiv (T - T_\infty)/(T_0 - T_\infty)$

Subscripts

0	=	at the body surface
∞	=	at points far from the body

Presented as Paper 94-1976 at the AIAA/ASME 6th Joint Thermophysics and Heat Transfer Conference, Colorado Springs, CO, June 20–23, 1994; received Aug. 19, 1994; revision received Dec. 19, 1994; accepted for publication Feb. 7, 1995. This paper was selected for the 1994 Best Thermophysics Paper Award.

*Professor and Director, Microelectronics Heat Transfer Laboratory, Department of Mechanical Engineering. Fellow AIAA.

†Research Engineer, Microelectronics Heat Transfer Laboratory, Department of Mechanical Engineering.

‡Research Associate Professor, Microelectronics Heat Transfer Laboratory, Department of Mechanical Engineering.

Introduction

COMPLETE solutions for transient heat conduction from most isothermal convex bodies, such as cuboids, short circular cylinders, and prolate and oblate spheroids, into a constant property medium of large extent over the full range of time values are currently not available in the literature. Although the solution of the transient temperature distribution in the region surrounding the oblate and prolate spheroids is theoretically possible as described by Morse and Feshbach,[1] the computation of heat flow rates from these bodies is prohibitively difficult because of the special functions that are required for the calculation. Norminton and Blackwell[2] and Blackwell[3] showed that it is possible to obtain long- and short-time expressions for the temperature distributions surrounding oblate and prolate spheroids. However, these authors do not report heat transfer rates for their short- and long-time solutions and they conclude that the exact solution for the complete problem seems impossibly difficult to obtain.

Solutions over the full-time range for the transient external problem for other convex body shapes, i.e., short circular cylinders or any cuboid bodies, are not available in any of the principal conduction texts.[1,4–6]

The only analytical, full-time, and easily implemented solution available for instantaneous heat flow from an isothermal convex body involves the sphere,[4] a limiting case of both the oblate and prolate spheroids. This simple solution combines the asymptotes corresponding to the short-time half-space solution and the long-time steady-state solution to develop a full-time expression.

Using the formulation suggested by the sphere solution, the following study proposes a simple and accurate model for predicting the dimensionless instantaneous heat flow rate from convex bodies of arbitrary shape. This model will implement the square root of the body's active surface area as the characteristic length to nondimensionalize both the heat flow rate and the time. It is anticipated that this choice of characteristic length will reduce all data to a single asymptote for short-time solutions and to a small range of values for long-time solutions. The proposed model will be applied to a wide range of body shapes, as presented in Fig. 1, including square disks, cubes and tall cuboids, the infi-

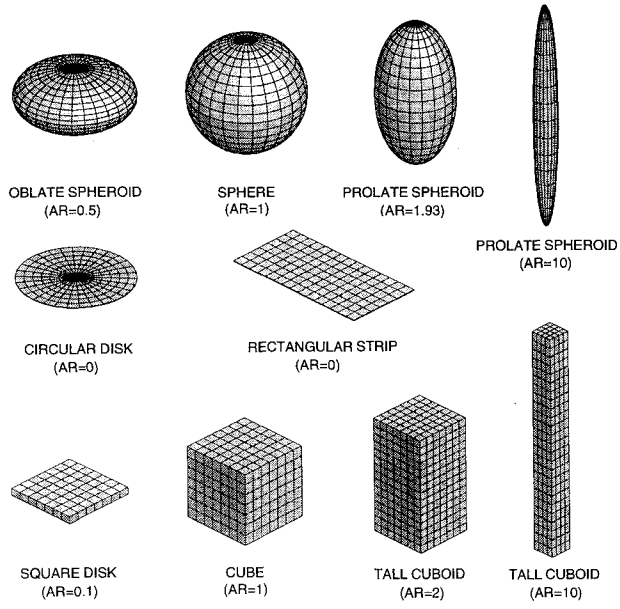

Fig. 1 Various convex body shapes for the transient external problem.

nitely thin circular disk and rectangular strip, and various oblate and prolate spheroids.

Because of the lack of analytical solutions in the literature for the transient external problem, the proposed model will be validated using numerical results from finite volume codes based in oblate spheroidal, prolate spheroidal, and Cartesian coordinates.

Problem Definition

The external problem, defined in this case as transient heat conduction from isothermal convex bodies of arbitrary shape into a constant property medium of large extent, can be characterized by the dimensionless heat flow rate Q^*_f. This quantity is available through the solution of the nondimensionalized diffusion equation in the surrounding region:

$$\nabla^2\phi(\boldsymbol{r}, \tau) = \frac{\partial\phi(\boldsymbol{r}, \tau)}{\partial\tau} \qquad \tau > 0, \qquad \boldsymbol{r} \geq \boldsymbol{r}_0 \tag{1}$$

where $\boldsymbol{r}_0$ defines the surface of the isothermal body. The dimensionless temperature excess for the surroundings, $\phi(\boldsymbol{r}, \tau)$, is defined as

$$\phi(\boldsymbol{r}, \tau) = [T(\boldsymbol{r}, \tau) - T_\infty]/(T_0 - T_\infty) \tag{2}$$

The nondimensional time τ is expressed in terms of a general characteristic length for the arbitrary convex body shape in question $\mathscr{L}$:

$$\tau = \alpha t/\mathscr{L}^2 \tag{3}$$

The initial and boundary conditions for Eq. (1) for the transient conduction problem in an infinitely large, uniform temperature medium with an isothermal boundary at the inner surface are

$$\phi(\boldsymbol{r}, 0) = 0 \tag{4}$$

$$\phi(\boldsymbol{r} = \boldsymbol{r}_0, \tau > 0) = 1 \tag{5}$$

$$\phi(\boldsymbol{r} \to \infty, \tau > 0) \to 0 \tag{6}$$

Using the solution to the diffusion equation $\phi(\boldsymbol{r}, \tau)$, the instantaneous heat flow rate Q from the isothermal body into the surroundings is determined by an area integration of the local heat flux at the inner boundary of the solution domain:

$$Q = k\theta_0 \iint_A -\nabla\phi\cdot\boldsymbol{n}\, dA \tag{7}$$

Nondimensionalizing this expression using the general characteristic length $\mathscr{L}$ yields

$$Q^*_f = \frac{Q\mathscr{L}}{kA\theta_0} = \frac{\mathscr{L}}{A_0}\iint_A -\nabla\phi\cdot\boldsymbol{n}\, dA \tag{8}$$

where θ_0 is the surface temperature difference, $T_0 - T_\infty$, and A is the active surface area of the body.

One of the objectives of this work is to propose a length scale that reduces the range of variation of the nondimensionalized heat flow rate, as expressed in Eq. (8), for all body shapes. The proper choice of $\mathscr{L}$ will minimize the dependence of this function on both the body's shape and aspect ratio.

There are many characteristic lengths that can be used for $\mathscr{L}$. For the example of the short circular cylinder, one may select either the diameter D or the height H, or various combinations of these two lengths such as $\mathscr{L} = V/A$, where V is the volume of the body and A is its total surface area. Other possible characteristic lengths may include either of the perimeter dimensions of the body, $\mathscr{L} = \pi D$ or $\mathscr{L} = 2D + 2H$. For the oblate and prolate spheroids, some researchers have used the semimajor and semiminor axis lengths. For spheres, the diameter is frequently chosen, while in the case of cubes, the side length is often selected.

However, when a general model for all body shapes is considered, the most appropriate body length has been found to be $\mathscr{L} = \sqrt{A}$, where A is the total heat transfer surface area of the body. It was first proposed by Yovanovich[7] for natural and forced convection heat transfer from single isothermal convex bodies of arbitrary shape. Chow and Yovanovich[8] demonstrated that when $\mathscr{L} = \sqrt{A}$ is used, the range of variation of the shape factor for the capacitance of conductors of arbitrary shape is minimized. This behavior of the capacitance shape factor is analogous to the steady-state, heat conduction shape factor for all body shapes.

In a similar manner, when $\mathscr{L} = \sqrt{A}$ is implemented at the short-time limit, the dimensionless instantaneous heat flow rates for all body shapes will collapse to a single asymptote corresponding to the classical half-space solution.

Using the proposed length scale $\mathscr{L} = \sqrt{A}$ and the transient temperature distribution[4] for the region surrounding an isothermal sphere of radius b

$$\phi(r, \tau) = \left(\frac{1}{r/b}\right)\operatorname{erfc}\left(\frac{r/b - 1}{4\sqrt{\pi}\sqrt{\tau}}\right) \tag{9}$$

the analytical solution for the dimensionless instantaneous heat flow rate from the isothermal sphere is determined by Eq. (8):

$$Q^*_{\sqrt{A}} = \frac{1}{\sqrt{A}}\iint_A \left\{-\frac{\partial}{\partial r}\left[\left(\frac{b}{r}\right)\operatorname{erfc}\left(\frac{r/b - 1}{4\sqrt{\pi Fo_{\sqrt{A}}}}\right)\right]\right\}_{r=b} dA$$
$$= 2\sqrt{\pi} + \frac{1}{\sqrt{\pi}\sqrt{Fo_{\sqrt{A}}}} \tag{10}$$

where the dimensionless time τ has been replaced by the more commonly used Fourier number:

$$Fo_{\sqrt{A}} = (\alpha t)/(\sqrt{A})^2 \tag{11}$$

The first term in Eq. (10) represents the long-time, steady-state asymptote corresponding to the conduction shape factor $S^*_{\sqrt{A}}$, and can be easily related to the dimensionless thermal resistance of the body $S^* = 1/R^*$. The second term in Eq.

(10) is the short-time asymptote that can be shown to be identical to the dimensionless heat flow rate of the semi-infinite solid solution. The resulting analytical expression for the transient heat flow rate from an isothermal sphere into the surrounding region is a simple linear superposition of these short- and long-time asymptotes.

Numerical Models

In order to examine the large number of body shapes for which the proposed superposition model is valid, two different numerical models are used. The first is a finite volume solution for the axisymmetric oblate and prolate spheroids, which includes as special cases the sphere and the infinitely thin, circular disk. The second numerical model used in this analysis is the commercial finite volume package FLOTHERM,[9] which, because of its use of Cartesian coordinates, will be used to model a variety of cuboid shapes. Both of these numerical formulations are briefly discussed in the following sections.

Oblate and Prolate Spheroid Models

The transient solution values for both the oblate and prolate spheroids are determined using a fully implicit, axisymmetric finite volume analysis for the region surrounding the isothermal body surface. The finite volume equation set for each of these cases is developed using the following formulation for an arbitrary control volume, as expressed in general orthogonal curvilinear coordinates[10]:

$$C_1 T_{i-1,j}^{m+1} + C_2 T_{i+1,j}^{m+1} + C_3 T_{i,j-1}^{m+1} + C_4 T_{i,j+1}^{m+1} + C_5 T_{i,j}^{m+1} = D \tag{12}$$

where the coefficients are determined using

$$C_{1,2} = \int_{u_3}\int_{u_2} \left(\frac{k\sqrt{g}}{g_{11}}\right)_{i\mp 1/2,j} \frac{du_2\, du_3}{(\Delta u_1)_{\mp}} \tag{13}$$

$$C_{3,4} = \int_{u_3}\int_{u_1} \left(\frac{k\sqrt{g}}{g_{22}}\right)_{i,j\mp 1/2} \frac{du_1\, du_3}{(\Delta u_2)_{\mp}} \tag{14}$$

$$C_5 = -\sum_{N=1}^{4} C_N - \rho c_p \frac{\Delta V}{\Delta t} \tag{15}$$

$$D = -\rho c_p \frac{\Delta V}{\Delta t} T_{i,j}^m \tag{16}$$

The notation i and j indicate control volume indices in the u_1 and u_2 directions, respectively, Δt is the time step, and ΔV is the volume of the control volume, determined using

$$\Delta V = \int_{u_3}\int_{u_2}\int_{u_1} \sqrt{g}\, du_1\, du_2\, du_3 \tag{17}$$

In order to apply this general formulation to the specific problem of an isothermal oblate spheroid, the following coordinate values are substituted into Eq. (12):

$$u_1 = \eta$$

$$u_2 = \theta$$

$$u_3 = \psi$$

as well as the metric coefficients[11]:

$$g_{11} = g_{22} = a^2(\cosh^2\eta - \sin^2\theta) \tag{18}$$

$$g_{33} = a^2 \cosh^2\eta \sin^2\theta \tag{19}$$

$$\sqrt{g} = a^3(\cosh^2\eta - \sin^2\theta)\cosh\eta \sin\theta \tag{20}$$

where a is the focal length of the body. After simplification, the finite volume coefficients for oblate spheroidal coordinates can be expressed as

$$C_{1,2} = \left[\frac{\cosh\eta_{i\mp 1/2,j}}{(\Delta\eta)_{\mp}} (\cos\theta_{i,j-1/2} - \cos\theta_{i,j+1/2})\right] \tag{21}$$

$$C_{3,4} = \left[\frac{\sin\theta_{i,j\mp 1/2}}{(\Delta\theta)_{\mp}} (\sinh\eta_{i+1/2,j} - \sinh\eta_{i-1/2,j})\right] \tag{22}$$

$$C_5 = -\sum_{N=1}^{4} C_N - \frac{\int_\theta\int_\eta \cosh\eta \sin\theta(\cosh^2\eta - \sin^2\theta)\, d\eta\, d\theta}{(\alpha t/a^2)} \tag{23}$$

$$D = -T_{i,j}^m \cdot \frac{\int_\theta\int_\eta \cosh\eta \sin\theta(\cosh^2\eta - \sin^2\theta)\, d\eta\, d\theta}{(\alpha t/a^2)} \tag{24}$$

where the integrals in Eqs. (23) and (24) must be evaluated numerically for each control volume in the solution domain (for a full derivation of the numerical model in oblate spheroidal coordinates, see Ref. 12).

Boundary conditions for the axisymmetric solution domain presented in Fig. 2 include adiabatic surfaces at $\theta = 0$ and $\theta = \pi$, as well as a homogeneous Dirichlet condition at $\eta \to \infty$ and an isothermal boundary at the body surface, where the coordinate position of this inner surface η_0 is related to the aspect ratio of the body AR by

$$\eta_0 = \tanh^{-1}(\mathrm{AR}) \tag{25}$$

This boundary moves between the limits $\eta = 0$ for the infinitely thin circular disk (AR = 0) and $\eta \to \infty$ for the sphere (AR = 1).

The finite volume equations for prolate spheroidal coordinates are determined from Eq. (12) in the same manner. By substituting

$$u_1 = \eta$$

$$u_2 = \theta$$

$$u_3 = \psi$$

and the metric coefficients[11]

$$g_{11} = g_{22} = a^2(\sinh^2\eta + \sin^2\theta) \tag{26}$$

$$g_{33} = a^2 \sinh^2\eta \sin^2\theta \tag{27}$$

$$\sqrt{g} = a^3(\sinh^2\eta + \sin^2\theta)\sinh\eta \sin\theta \tag{28}$$

the finite volume coefficients become

$$C_{1,2} = \left[\frac{\sinh\eta_{i\mp 1/2,j}}{(\Delta\eta)_{\mp}} (\cos\theta_{i,j-1/2} - \cos\theta_{i,j+1/2})\right] \tag{29}$$

$$C_{3,4} = \left[\frac{\sin\theta_{i,j\mp 1/2}}{(\Delta\theta)_{\mp}} (\cosh\eta_{i+1/2,j} - \cosh\eta_{i-1/2,j})\right] \tag{30}$$

$$C_5 = -\sum_{N=1}^{4} C_N - \frac{\int_\theta\int_\eta \sinh\eta \sin\theta(\sinh^2\eta + \sin^2\theta)\, d\eta\, d\theta}{(\alpha t/a^2)} \tag{31}$$

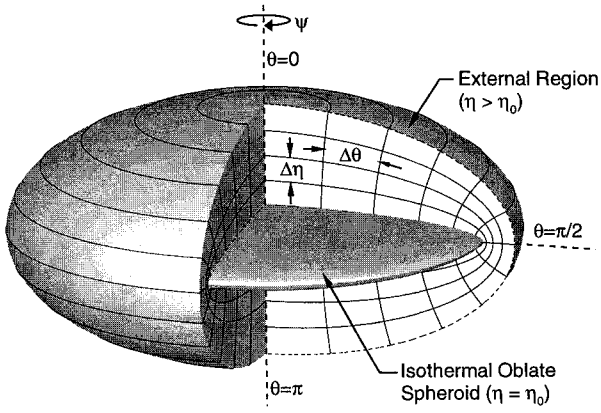

Fig. 2 Finite volume model in oblate spheroidal coordinates.

$$D = -T^{m}_{i,j} \cdot \frac{\int_{\theta}\int_{\eta} \sinh\eta \sin\theta(\sinh^2\eta + \sin^2\theta)\, d\eta\, d\theta}{(\alpha t/a^2)} \quad (32)$$

Boundary conditions in the solution domain are similar to those presented for the oblate spheroid problem, with the exception of the coordinate value of the isothermal inner surface, determined in this case using

$$\eta_0 = \tanh^{-1}(1/\mathrm{AR}) \quad (33)$$

This numerical model has been validated for a number of limiting cases, including the full-time sphere and long-time[2] and short-time[3] circular disks (for a full description of this validation, see Ref. 12). For the sphere problem, differences between the numerical values and the exact solution is less than 1%, while the numerical results for the circular disk varied from the long- and short-time approximations by less than 2% within their applicable ranges of dimensionless time.

Cuboid Models

The transient numerical solutions for all cuboid shapes are determined using the FLOTHERM computational fluid dynamics (CFD) software. Because of the symmetry that occurs in all three planes of the three-dimensional bodies, the origin of the local Cartesian coordinate system is placed at the center of the body and adiabatic planes are introduced at $x = 0$, $y = 0$, and $z = 0$, resulting in a model that represents one-eighth of the total volume of the body. The boundary condition on the inner surface of the solution domain is a cuboid-shaped, isothermal heat source placed at $0 \le x \le s_1$, $0 \le y \le s_2$, and $0 \le z \le s_3$, where s_1, s_2, and s_3 are the half-lengths of the sides of the body. This boundary condition and the solution domain discretization are presented in Fig. 3.

In order to effectively model an at-infinity homogeneous Dirichlet boundary condition for the transient conduction solution, a number of different solution domain discretizations were used. For short-time problems, $Fo_{\sqrt{A}} \approx 10^{-5}$–$10^{-4}$, where it is anticipated that the temperature field will remain very close to the body, the depth of the solution domain is kept at a level close to the side length of the body, and a large number of very thin control volumes are placed near the isothermal surface. As the transient solution progresses, the outer boundary is moved outward until the long-time limit is reached, $Fo_{\sqrt{A}} \approx 10^{2}$–$10^{3}$, where the required field depth is of order 50 times the side length of the body. In order to keep the model size to a minimum, especially for the long-time cases, special grid-generation techniques within the CFD software are implemented that concentrate control volumes near the isothermal body surface, as shown in Fig. 3.

The numerical results for the cuboids have been validated using both the half-space asymptote as well as the steady-state

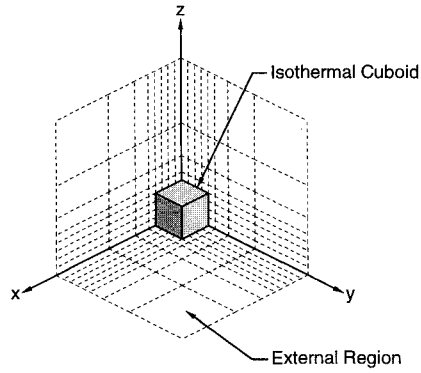

Fig. 3 Finite volume model for cuboids in Cartesian coordinates.

conduction shape factor for a number of bodies with an aspect ratio near unity. Although accuracy for the short-time problems seemed to suffer as a result of the roundoff error associated with large temperature gradients near the body surface, the steady-state numerical model was able to predict the conduction shape factor for the cube, the square disk (AR = 0.1) and the tall cuboid (AR = 2) to within 1% of the values presented by Martin.[13]

Results

Numerical Results

The numerical results for the transient temperature distribution in the homogeneous medium surrounding the isothermal bodies, obtained by means of the two finite volume methods, have been reduced into time-dependent, dimensionless heat flow rates using

$$Q^{*}_{\sqrt{A}} = \frac{1}{\sqrt{A}} \int\int_{A} -\nabla\phi \cdot \boldsymbol{n}\, dA \quad (34)$$

For the oblate and prolate spheroids, including the circular disk, this area-mean heat flux expression becomes

$$Q^{*}_{\sqrt{A}} = \frac{1}{(T_0 - T_\infty)\sqrt{A}} \int_{\psi}\int_{\theta} \left[\frac{\sqrt{g}}{g_{11}}\left(-\frac{\partial T}{\partial \eta}\right)\right]_{\eta=\eta_0} d\theta\, d\psi \quad (35)$$

where the temperature gradient at the body surface is available through a first-order approximation of the numerical results.

For the case of the cuboids, the integral in Eq. (34) must be evaluated in a piecewise manner for each surface of the body. For the FLOTHERM model used in the present analysis, symmetry allows the evaluation of the shape factor using only a small portion of the total surface area of the body:

$$Q^{*}_{\sqrt{A}} = \frac{1}{(T_0 - T_\infty)\sqrt{A}} \left[\int_0^{s_3}\int_0^{s_2} -\left.\frac{\partial T}{\partial x}\right|_{x=s_1} dy\, dz + \int_0^{s_3}\int_0^{s_1} -\left.\frac{\partial T}{\partial y}\right|_{y=s_2} dx\, dz + \int_0^{s_2}\int_0^{s_1} -\left.\frac{\partial T}{\partial z}\right|_{z=s_3} dx\, dy\right] \quad (36)$$

where s_1, s_2, and s_3 are the half-lengths of the body in the x, y, and z directions, and

$$A = (s_1 \times s_2) + (s_1 \times s_3) + (s_2 \times s_3) \quad (37)$$

The dimensionless instantaneous heat flow rates $Q^{*}_{\sqrt{A}}$ for 10 body shapes have been plotted for the full range of dimensionless time $10^{-6} < Fo_{\sqrt{A}} < 10^{3}$ in Fig. 4. These numerical results include a wide range of body shapes, such as

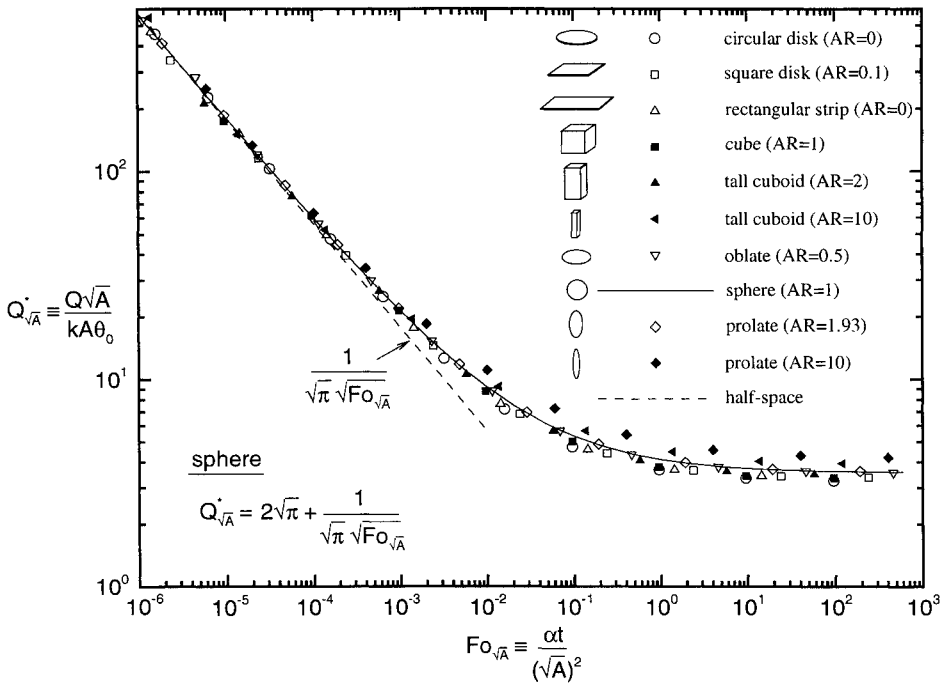

Fig. 4 Sphere analytical solution and numerical results for external transient conduction from various body shapes.

the thin circular and square disks, the sphere and cube, the oblate and prolate spheroids, and the tall square cuboid. All these body shapes have a large variation in aspect ratio, spanning the range $0 \leq AR \leq 10$.

As can be seen from Fig. 4, all values of $Q^*_{\sqrt{A}}$ for all body shapes are in excellent agreement with the half-space asymptote provided $Fo_{\sqrt{A}} < 10^{-4}$. In addition, it can be shown that the numerical results for all bodies follow the trend of the sphere solution, with values that are very close to the sphere over the entire range of dimensionless time. The results for the oblate and prolate spheroids and the sphere are almost identical over the entire range of $Fo_{\sqrt{A}}$. The maximum differences are observed between the thin bodies (circular and square disks) and the tall bodies (prolate spheroid AR = 10 and the tall cuboid AR = 10). These differences, which occur between the steady-state asymptotes, are approximately 25%.

Linear Superposition Model

The proposed superposition model for the instantaneous dimensionless heat flow is

$$Q^*_{\sqrt{A}} = S^*_{\sqrt{A}} + [1/(\sqrt{\pi}\sqrt{Fo_{\sqrt{A}}})] \tag{38}$$

where $S^*_{\sqrt{A}}$ is the dimensionless conduction shape factor for isothermal bodies of arbitrary shape. The values used for $S^*_{\sqrt{A}}$ in the present analysis are based on results and models found in several references.[7,8,14-17] Table 1 presents a comparison of the results of the model with the numerical results for the nine nonspherical body shapes in terms of the maximum and rms percent difference. As can be seen from these results, the superposition model shows good agreement with the numerical values for bodies with aspect ratios close to unity, such as the square disk, the cube, the tall cuboid (AR = 2), and the oblate (AR = 0.5) and prolate (AR = 1.93) spheroids. However, in the case of bodies with very large or very small aspect ratios, AR >> 1 or AR → 0, large inaccuracies in the model may occur in the intermediate range, $10^{-3} < Fo_{\sqrt{A}} < 10^{-1}$.

Blended Superposition Model

In order to improve the effectiveness of the model for all body shapes regardless of their aspect ratio, blending is applied using the Churchill and Usagi method[18] to the short- and long-time asymptotes. By introducing the blending parameter n, the superposition model can be expressed as

$$(Q^*_{\sqrt{A}})^n = (S^*_{\sqrt{A}})^n + [1/(\sqrt{\pi}\sqrt{Fo_{\sqrt{A}}})^n] \tag{39}$$

where, in the case of no blending ($n = 1$), the model is reduced to a linear superposition of the asymptotes, corresponding to Eq. (38). Rearranging the blended expression yields an explicit formulation for the instantaneous dimensionless heat flow:

$$Q^*_{\sqrt{A}} = [1/(\sqrt{\pi}\sqrt{Fo_{\sqrt{A}}})]\{\{S^*_{\sqrt{A}}/[1/(\sqrt{\pi}\sqrt{Fo_{\sqrt{A}}})]\}^n + 1\}^{1/n} \tag{40}$$

where Eq. (39) has been arbitrarily expanded in terms of the half-space asymptote. Introducing a blending parameter $n \neq 1$ in the preceding equation will not effect the values predicted for the short- or long-time limits, but in the intermediate range, $10^{-3} < Fo_{\sqrt{A}} < 10^{-1}$, small changes in n will have a large effect on the results. Values of $n > 1$ will tend to decrease the value of the function in the midrange, while $n < 1$ increases its value.

Table 2 compares the numerical results for the nine body shapes presented in Table 1 with the values predicted by the blended solution, where a blending parameter has been determined for each case, which minimizes the rms percent difference. It is obvious from Table 2 that applying blending to the superposition model has greatly increased the accuracy, especially for cases where AR → 0, such as the circular disk or rectangular strip, or AR >> 1, such as the tall cuboid or prolate (AR = 10). Using the optimized blending parameter in each case leads to an rms percent difference between the numerical results and the model of less than 1% for most cases.

In order to apply the blended model to an arbitrary body shape where the solution is not known, it is necessary to examine the trends evident in both Fig. 4 and Table 2 in order to make some recommendations concerning the proper choice of blending parameter. A general recommendation would be that bodies with small aspect ratios, such as disks and thin plates, require blending parameters that are larger than 1,

Table 1 Comparison of superposition model and numerical results

Body	$S^*_{\sqrt{A}}$	% difference Maximum	% difference rms
Circular disk (AR = 0)	3.192	7.05	3.36
Rectangular strip (AR = 0)	3.303	4.99	2.94
Square disk (AR = 0.1)	3.343	2.60	1.91
Cube (AR = 1)	3.388	3.78	2.52
Tall cuboid (AR = 2)	3.406	2.77	1.87
Oblate spheroid (AR = 0.5)	3.529	0.98	0.40
Prolate spheroid (AR = 1.93)	3.564	1.65	0.73
Tall cuboid (AR = 10)	3.945	3.15	1.63
Prolate spheroid (AR = 10)	4.195	11.52	6.31

Table 2 Comparison of blended model and numerical results

Body	n	% difference Maximum	% difference rms
Circular disk (AR = 0)	1.10	1.83	0.80
Rectangular strip (AR = 0)	1.07	1.28	0.62
Square disk (AR = 0.1)	1.05	1.44	0.67
Cube (AR = 1)	1.05	1.95	1.04
Tall cuboid (AR = 2)	1.03	1.65	0.81
Oblate spheroid (AR = 0.5)	0.99	0.82	0.36
Prolate spheroid (AR = 1.93)	0.99	1.59	0.53
Tall cuboid (AR = 10)	0.96	2.08	1.13
Prolate spheroid (AR = 10)	0.87	2.06	1.34

Table 3 Blending parameter recommendations

Body	Aspect ratio	n
Spheroids		
Infinitely thin disk	AR $\approx$ 0	1.1
Oblates and prolates	0.5 < AR < 2	1.0
Tall prolates	2 < AR < 10	0.9
Cuboids		
Infinitely thin disk	AR $\approx$ 0	1.07
Thin disks and cubes	0.1 < AR < 1	1.05
Tall cuboids	AR $\approx$ 2	1.03
Square cylinders	2 < AR < 10	0.96

while bodies with large aspect ratios need blending parameters smaller than 1. More specific recommendations are presented in Table 3. These blending parameters have been recommended based on the numerical results, and as such, may contain inaccuracies due to errors and approximations in the finite volume solutions.

Conclusions

A model for full-time solutions for transient heat conduction from isothermal convex bodies has been developed by combining the short- and long-time asymptotes, corresponding to the half-space solution and the conduction shape factor. It has been demonstrated that by using the square root of the active body surface area as the characteristic body length in nondimensionalizing the time and heat flow quantities, all short-time values for arbitrary convex bodies are reduced to a single asymptote. In the case of long-time values, the use of this characteristic length has been shown to greatly reduce the range of variation of the conduction shape factor for all body shapes. The linear superposition model, when compared to numerical full-time results for a wide variety of body shapes and aspect ratios, gave good agreement for bodies with aspect ratios near unity, but showed larger variations for very thin or very tall bodies. In order to increase the accuracy of the model for these extreme cases a blended superposition model was introduced, resulting in a significant improvement in the agreement between the model and the numerical values over the range of bodies tested. Recommended values for this blending parameter have been presented as a function of both the aspect ratio and body shape.

Acknowledgments

The authors gratefully acknowledge the support of the Natural Sciences and Engineering Research Council of Canada under Operating Grant 661-069/91 for M. M. Yovanovich.

References

[1]Morse, P. M., and Feshbach, H., *Methods of Theoretical Physics*, Part I–II, McGraw–Hill, New York, 1953.

[2]Norminton, E. J., and Blackwell, J. H., "Transient Heat Flow from Constant Temperature Spheroids and the Thin Circular Disk," *Quarterly Journal of Mechanics and Applied Mathematics*, Vol. 17, Pt. 1, 1964, pp. 65–72.

[3]Blackwell, J. H., "Transient Heat Flow from a Thin Circular Disk—Small-Time Solution," *Journal of the Australian Mathematical Society*, Vol. 14, 1972, pp. 433–442.

[4]Carslaw, H. S., and Jaeger, J. C., *Conduction of Heat in Solids*, 2nd ed., Clarendon, Oxford, England, UK, 1959.

[5]Ozisik, M. N., *Heat Conduction*, Wiley, New York, 1980.

[6]Hill, J. M., and Dewynne, J. N., *Heat Conduction*, Blackwell Scientific Publications, Palo Alto, CA, 1987.

[7]Yovanovich, M. M., "New Nusselt and Sherwood Numbers for Arbitrary Isopotential Geometries at Zero Peclet and Rayleigh Numbers," AIAA Paper 87-1643, June 1987.

[8]Chow, Y. L., and Yovanovich, M. M., "The Shape Factor of the Capacitance of a Conductor," *Journal of Applied Physics*, Vol. 53, No. 12, 1982, pp. 8470–8475.

[9]FLOTHERM, Flomerics Inc., Westborough, MA, 1994.

[10]Schneider, G. E., "Discrete Methods in Heat Conduction: A Review," *Advances in Transport Processes*, Vol. 3, edited by A. S. Mujumdar and R. A. Mashelkar, Wiley Eastern, New Delhi, India, 1984, pp. 122–130.

[11]Moon, P., and Spencer, D. E., *Field Theory Handbook*, Springer–Verlag, Berlin, 1961.

[12]Teertstra, P., "Heat Conduction in Regions Surrounding Oblate Spheroidal Bodies," M.Sc. Thesis, Univ. of Waterloo, Waterloo, Ontario, Canada, 1992.

[13]Martin, K. A., through personal communication with M. M. Yovanovich, Univ. of Waterloo, Ontario, Canada, 1980.

[14]Hahne, E., and Grigull, U., "Formfaktor und Formwiderstand der Stationaren Mehrdimensionalen Warme-leitung," *International Journal of Heat and Mass Transfer*, Vol. 18, No. 6, 1975, pp. 751–767.

[15]Hahne, E., and Grigull, U., "A Shape Factor Scheme for Point Source Configurations," *International Journal of Heat and Mass Transfer*, Vol. 17, No. 2, 1975, pp. 267–272.

[16]Smythe, W. R., "Charged Right Circular Cylinder," *Journal of Applied Physics*, Vol. 27, No. 8, 1956, pp. 917–920.

[17]Smythe, W. R., "Charged Right Circular Cylinder," *Journal of Applied Physics*, Vol. 33, No. 10, 1962, pp. 2966, 2967.

[18]Churchill, S. W., and Usagi, R., "A General Expression for the Correlation of Rates and Other Phenomena," *American Institute of Chemical Engineers Journal*, Vol. 18, No. 6, 1972, pp. 1121–1132.